EUROPEAN ORGANIZATION FOR NUCLEAR RESEARCH

CERN–EP/98-125
7 August 1998

Laser spectroscopy investigation of the nuclear moments and radii of lutetium isotopes

U. Georg[a)], W. Borchers[b)], M. Keim[*)], A. Klein[c)], R. Neugart, M. Neuroth[d)], C. Schulz[e)]
Institut für Physik, Universität Mainz, D-55099 Mainz, Germany.

Pushpa M. Rao
Spectroscopy Division, Bhabha Atomic Research Centre, Bombay, India.

P. Lievens[f)] the ISOLDE Collaboration
EP Division, CERN, CH-1211 Geneva 23, Switzerland.

Abstract

Collinear laser spectroscopy experiments in the LuI transition $5d6s^2\ ^2D_{3/2} \rightarrow 5d6s6p\ ^2D_{3/2}$ were performed on all lutetium isotopes in the range of $^{161-179}$Lu. The nuclear spins, magnetic moments and quadrupole moments were determined from the hyperfine structures observed for 19 ground states and 11 isomers. Variations in the mean square charge radii as a function of neutron number were obtained from the isotope shifts. These data considerably extend the systematics of the properties of nuclei in the upper rare-earth region. A particular feature is the appearance of high-spin and low-spin ground states and isomeric states in the vicinity of the stable ^{175}Lu, partly arising from aligned neutron pairs. The present results clearly show that the deformation properties are nearly independent of the occupancy and the coupling of single-particle states. Theoretical predictions of deformation are confirmed in a consistent description of the measured radii and quadrupole moments. For all observed states, the spins and magnetic moments allow the assignment of rather pure Nilsson configurations.

(Submitted to European Physical Journal A)

[a)] Present address: EP Division, CERN, CH-1211 Geneva 23, Switzerland
[b)] Present address: Agfa-Gevaert AG, D-51301 Leverkusen.
[c)] Present address: Zimmer AG, Borsigallee 1, D-60388 Frankfurt.
[d)] Present address: Ungerer Meßtechnik GmbH & Co, D-75179 Pforzheim.
[e)] Present address: Siemens Nixdorf Informationssysteme AG, D-60528 Frankfurt.
[f)] Now Postdoctoral Researcher of the Fund for Scientific Research – Flanders (F.W.O.) at the Laboratorium voor Vaste-Stoffysica en Magnetisme, K.U. Leuven, B-3001 Leuven, Belgium.

1 Introduction

For many years laser spectroscopy has been used to gain information on nuclear ground-state properties. Particularly in the rare-earth region the systematics of mean square charge radii, spins, magnetic moments and quadrupole moments, usually available for strings of isotopes, has been extended over a considerable range of proton numbers [1, 2]. This means that the development of nuclear shapes, as well as the occupancy of single-particle orbitals forming the nuclear ground states and the longer-lived isomers, can be mapped in a two-dimensional region of the chart of nuclides. Lutetium ($Z = 71$) is situated at the upper end of a sequence of elements that are available in the form of ion beams at on-line isotope separator facilities and are as well suitable for high-resolution laser spectroscopy experiments.

So far, atomic spectroscopy work yielding nuclear moments and isotope shifts of lutetium isotopes has remained rather scarce. This is due to the former lack of isotope production schemes suitable for preparing samples of free atoms. Only two isotopes, the stable ^{175}Lu and the very long-lived ^{176}Lu, are occuring in nature. Cyclotron-produced samples of most radioactive isotopes were too small as to allow complete hyperfine structure studies. Moreover, the short half-lives of isotopes far from stability require special on-line techniques.

First investigations using the atomic beam magnetic resonance (ABMR) technique with reactor-produced long-lived isotopes were reported in the early sixties [3, 4]. They yielded the spins, the magnetic moments and the quadrupole moments of ^{176m}Lu and ^{177}Lu. Later on, a number of additional spins of cyclotron-produced neutron-deficient isotopes were determined by Ekström [5]. A few ground states and isomers close to stability were investigated with the help of low-temperature nuclear orientation. The history and the insufficiencies of this early nuclear orientation work has been discussed by König et al. [7] who performed very careful magnetic resonance experiments on low-temperature oriented nuclei implanted into cobalt single crystals. These new experiments yielded reliable values of the magnetic moments as well as the unknown quadrupole moments of (altogether seven) typical candidates for off-line nuclear orientation.

We report on a more extended laser spectroscopy investigation[1)] of hyperfine structures and isotope shifts, which has been performed essentially in parallel to the recent nuclear orientation work [7]. Apart from covering all isotopes investigated previously, our results include the magnetic moments and quadrupole moments of eleven ground states and eight isomers not investigated before. Moreover, they provide valuable complementary information on the nuclear mean square charge radii which is obtained from the isotope (isomer) shifts. Previously, optical isotope shift measurements had been restricted to the naturally occuring isotopes ^{175}Lu and ^{176}Lu [9, 10].

2 Experimental Setup and Measurements

The experiments were carried out at the ISOLDE on-line mass separator facility at CERN. Lutetium isotopes were produced in spallation reactions induced by the 600 MeV proton beam from the Synchro-Cyclotron in a 120 g/cm^2 target of stacked rolls of tantalum foils [11]. The target which is heated at about 2000 ^{0}C releases neutron-deficient isotopes of nearly all rare-earth elements including lutetium which is produced according to ^{181}Ta (p, 3pxn) $^{179-x}$Lu. Ionization takes place on a hot tungsten surface, and the ions are accelerated by a static voltage of 60 kV. After magnetic mass-separation the ions are guided into the apparatus for collinear laser spectroscopy [12].

[1)] Preliminary results were already reported in ref. [8]

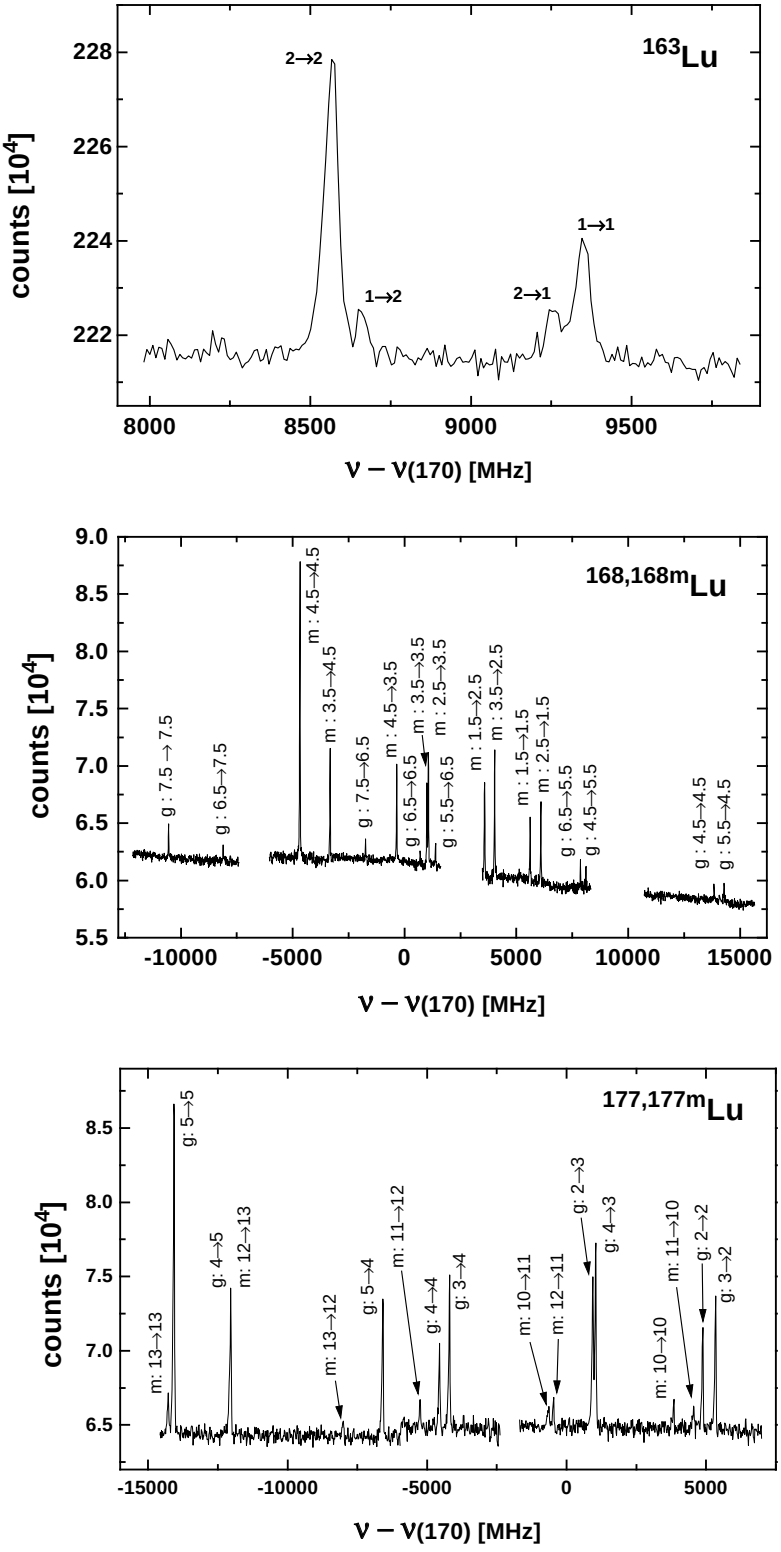

Figure 1: Spectra of the hyperfine structure of selected isotopes: a) ^{163}Lu with $I = 1/2$; b) ^{168}Lu ($I = 6$) and ^{168m}Lu ($I = 3$); c) ^{177}Lu ($I = 7/2$) and ^{177m}Lu ($I = 23/2$). The common reference position is the single line of ^{170}Lu ($I = 0$). The spectra spanning ranges of about 25 GHz are divided into several scans.

The ion beam merged with the laser beam from a cw dye laser system is travelling through a sodium-vapour cell where neutral atoms in the ground state are formed in peripheral charge-exchange collisions. With the laser at resonance, fluorescence photons are emitted along the beam path. These are collected and guided to the cathode of a single-photon multiplier with the help of large-aperture mirrors and lenses and a light pipe. The Doppler-shifted optical frequency is varied by post-accelerating or -decelerating the ions prior to neutralization, while the laser frequency is kept constant (Doppler-tuning).

Optical spectroscopy with the unique sensitivity and resolution features of the collinear laser-fast beam technique was performed in the resonance transition from the $5d6s^2\ ^2D_{3/2}$ atomic ground state to the $5d6s6p\ ^2D_{3/2}$ excited state at the (rest frame) wavelength of 451.9 nm. The laser system was operated with the dye Stilben 3 pumped by the UV lines of an argon-ion laser. Since fluorescence occurs predominantly at the same wavelength, the photon collection optics was used without any blocking filters, thus being sensitive to stray laser light and some background due to collisional excitation of the atoms. This latter background is not only due to lutetium, but mostly to the isobars of the neighbouring rare-earth elements which are present in the beams [11]. It was kept at a tolerable level in the range of $10 - 100$ kHz depending on the isobar mass by running the charge exchange cell at a relatively low sodium vapour pressure and by using a blue-sensitive photo multiplier. Compared to this, the stray light background of a few kHz plays a minor role for most of the isotopes except for the heaviest which are available as rather pure beams.

Three examples selected from the large number of hyperfine structure spectra are presented in Figure 1. The frequency scale gives the distance from the single line of ^{170}Lu which has the nuclear spin $I = 0$. Figure 1.a) on ^{163}Lu represents the $I = 1/2$ spectra found for the lightest odd-A isotopes (^{161}Lu, ^{163}Lu and ^{165}Lu) for which no isomers were observed. All other spectra, spanning tens of GHz, are composed of a number of narrower scans. This measuring mode was chosen in order not to risk laser mode hops or drifts that could occur during data acquisition times of many hours. Usually the hyperfine structure components belonging to the nuclear ground and isomeric states are about equally strong, meaning that the production rates are about the same. Such examples are given in Figure 1.b) for the case of ^{168}Lu ($I = 6$) and ^{168m}Lu ($I = 3$) and in Figure 1.c) for the case of ^{177}Lu ($I = 7/2$) and ^{177m}Lu ($I = 23/2$). The total angular momentum quantum numbers F are indicated for all individual lines that are visible in the spectrum.

These spectra were originally taken as a function of the acceleration voltage with respect to a reference line of one particular isotope (usually ^{170}Lu). By calculating relative Doppler shifts based on the Wapstra mass tables [13] it is thus possible to establish a common frequency scale for all measurements. For technical reasons, the general reference isotope ^{170}Lu was abandoned in a few cases, and either ^{166m}Lu ($I = 0$) or the strongest hyperfine structure component of ^{165}Lu ($I = 1/2$) served as a secondary reference.

The hyperfine structure of an atomic level is described by the magnetic dipole interaction parameter A and the electric quadrupole interaction parameter B and depends on the angular momenta involved, J for the shell electron state and I for the nucleus, coupled to the total angular momentum F:

$$\Delta\nu_{\rm hfs} = \frac{1}{2}KA + \frac{\frac{3}{4}K(K+1) - J(J+1)I(I+1)}{2I(2I-1)(2J-1)}B\,, \qquad (1)$$

with $\qquad K = F(F+1) - I(I+1) - J(J+1)\,.$

This formula holds independently for the lower and the upper state of the transition, with differ-

Table 1: A- and B-factors of the hyperfine structure in the $5d6s^2\,^2D_{3/2}$ ground state and the $5d6s6p\,^2D_{3/2}$ excited state obtained from the least-squares fits of formula (1) to the measured transition lines. Only the dominant parameters A_e and B_g are given for the cases in which prefixed ratios A_e/A_g and B_e/B_g were used. These are marked with asterisks.

Isotope	I	A_g [MHz]	A_e [MHz]	B_g [MHz]	B_e [MHz]	Ref.
161*	1/2		-998.3 (1.5)	-	-	
162*	1		-123.6 (1.2)	225 (3)		
163*	1/2		-343.4 (1.0)	-	-	
164*	1		-132.1 (1.0)	264 (3)		
165*	1/2		109.6 (2)	-	-	
166	6	147.8 (6)	-1083.8 (6)	1877 (10)	-601 (9)	
$166m_1$	3	19.2 (5)	-142.0 (6)	1176 (4)	-391 (4)	
$166m_2$	0	-	-	-	-	
167	7/2	202.4 (3)	-1483.8 (4)	1418 (3)	-469 (3)	
167m*	1/2		446.3 (1.4)	-	-	
168	6	153.1 (1.3)	-1116.8 (1.2)	2064 (18)	-710 (19)	
168m	3	124.0 (5)	-902.7 (5)	1053 (4)	-343 (3)	
169	7/2	199.8 (3)	-1465.1 (3)	1507 (3)	-496 (3)	
169m*	1/2		-2404(7)	-	-	
170	0	-	-	-	-	
171	7/2	199.6 (4)	-1464.4 (4)	1527 (3)	-505 (3)	
171m*	1/2		-2615(4)	-	-	
172	4	220.9 (8)	-1616.3 (8)	1644 (8)	-539 (8)	
172m	1	603 (11)	-4444 (11)	327 (11)	-116 (11)	
173	7/2	198.51 (18)	-1455.1 (2)	1529.2 (1.6)	-502.5 (1.8)	
174	1	605.8 (1.3)	-4420.2 (1.2)	334.9 (1.6)	-111.0 (1.6)	
174m	6	75.7 (9)	-554.0 (8)	2078 (13)	-689 (11)	
175	7/2	194.4 (7)	-1424.7 (7)	1509 (6)	-501 (6)	
		194.33162(9)		1511.39865(69)		[16]
176	7	137.6 (5)	-1006.5 (6)	2132 (11)	-698 (13)	
		137.92054(12)		2132.2969(25)		[16]
176m	1	95 (2)	-708 (2)	-628 (3)	219 (3)	
		97.19644(30)		-635.19314(70)		[4]
177	7/2	194.9 (6)	-1428.9 (7)	1467 (5)	-484 (6)	
		194.84 (2)		1466.71 (12)		[3]
177m	23/2	61.2 (3)	-448.0 (4)	2472 (11)	-807 (12)	
178	1	-419 (3)	3078 (3)	307 (4)	-104 (4)	
178m	9	163.6 (4)	-1188.4 (4)	2333 (11)	-758 (11)	
179	7/2	206.8 (1.0)	-1515.6 (1.2)	1436 (8)	-465 (8)	

Table 2: Isotope shifts and differences of mean square charge radii compared to ^{170}Lu. A few isotope shifts were deduced from measurements using a different reference isotope (indicated in column 4). Statistical errors (in parentheses) and systematic errors (in square brackets) are given separately[a]. The differences of mean square radii are subject to a 10 % general calibration error[b]. Experimental errors are smaller than one unit in the last digit.

Isotope A'	I	$\delta\nu^{A,A'}$ [MHz]	A	$\delta\nu^{170,A'}$ [MHz]	$\delta\langle r^2\rangle^{170,A'}$ [fm^2]
161	1/2		170	11892 (6)[6]	-1.120
162	1		170	10733 (5)[6]	-1.011
163	1/2		170	8866 (3)[5]	-0.835
164	1		170	7653 (2)[4]	-0.721
165	1/2		170	5950.3 (1.3)[3.6]	-0.561
166	6	-385.6 (2.9)[0.5]	166m$_2$	4366 (3)[3]	-0.412
166m$_1$	3	-46.6 (1.6)[0.5]	166m$_2$	4705.2 (1.7)[3.4]	-0.444
166m$_2$	0		170	4751.7 (0.6)[3.2]	-0.448
167	7/2	-3097.1 (1.3)[2.2]	165	2853.2 (1.8)[2.9]	-0.269
167m	1/2	-2866 (4)[2]	165	3085 (4)[3]	-0.291
168	6	-3223 (6)[2]	166m$_2$	1529 (6)[2]	-0.144
168m	3	-4495.9 (1.3)[2.6]	166m$_2$	255.9 (1.4)[2.2]	-0.024
169	7/2	-3925.0 (1.1)[2.7]	166m$_2$	826.8 (1.2)[1.9]	-0.078
169m	1/2	-6128 (7)[3]	166m$_2$	-1377 (7)[2]	0.130
170	0		170	0	0
171	7/2	-5559.2 (1.2)[3.6]	166m$_2$	-807.4 (1.3)[2.2]	0.076
171m	1/2	-8247 (6)[4]	166m$_2$	-3496 (5)[3]	0.330
172	4		170	-1362 (3)[2]	0.129
172m	1		170	-1276 (7)[2]	0.120
173	7/2		170	-2381.4 (7)[2.1]	0.225
174	1		170	-3022.7 (1.7)[2.5]	0.286
174m	6		170	-3019 (3)[3]	0.285
175	7/2		170	-3765 (3)[3]	0.356
176	7		170	-4200 (4)[4]	0.397
176m	1		170	-4315 (3)[4]	0.408
177	7/2		170	-5052 (3)[4]	0.477
177m	23/2		170	-4672 (4)[4]	0.442
178	1		170	-5530 (4)[4]	0.523
178m	9		170	-6333 (3)[4]	0.599
179	7/2		170	-6194 (4)[5]	0.586

[a] In calculating the isotope shifts for any pair of isotopes the quoted errors should be treated as follows: (*i*) Statistical errors should be added up quadratically; (*ii*) Systematic errors should be added or subtracted linearly in the same manner as the absolute values of the isotope shifts. 1 MHz should be added to allow for rounding errors, and the resulting error should not fall below 2 MHz. For isomer shifts (differences between isomer and ground state of the same nucleus) the systematic errors are practically negligible.

[b] Relative values of $\delta\langle r^2\rangle$ are largely free from the calibration uncertainties introduced by the electronic factor and the mass shift correction.

ent A- and B-factors, A_g, B_g and A_e, B_e, respectively. The centroids of both hyperfine structure multiplets define the line positions entering into the determination of isotope shifts. The number of observable hyperfine structure components, determined by the dipole selection rules, is usually larger than the number of independent parameters.

According to this, the isotope shifts and the hyperfine structure parameters were evaluated using the program MINUIT [14] by running a least-squares fit over all observed lines of an isotope. In a few cases (see Table 1) the number of observed or resolved lines was not sufficient for extracting the ground-state and excited-state A- and B-factors independently. Then the ratios A_e/A_g and B_e/B_g, which are independent of the nuclear properties apart from small hyperfine anomaly effects, were fixed at $A_e/A_g = -7.331(4)$ and $B_e/B_g = -0.330(1)$. These ratios are the average values obtained from the other isotopes. They are in very good agreement with the results obtained by Engleman et al. [15] for the stable ^{175}Lu, $A_e/A_g = -7.3316(3)$ and $B_e/B_g = -0.3301(6)$.

The nuclear spins and the A- and B-factors resulting from this analysis are compiled in Table 1, together with results of the earlier measurements quoted in Section 1. The isotope shifts, i.e. the distances of the centers of gravity from the single line of ^{170}Lu with $I = 0$ are given in Table 2, column 5. For measurements using different reference isotopes the direct result is additionally given in column 3, with the reference isotope shown in column 4. The errors of the isotope shifts contain a statistical and a systematic contribution. The systematic error, quoted separately, is caused by the 10^{-4} uncertainty of the voltage measurements entering into the calculation of Doppler shift differences. The error evaluation procedure has been described in the paper by Mueller et al. [12].

3 The Nuclear Spins and Moments

As shown above, the nuclear spins are directly obtained from the least-squares fits which reproduce the observed spectra only with the correct assumption for the spin values. In doubtful cases all other possible spins were ruled out by the pertinent statistical checks.

The values of μ_I were calculated from the A-factors, using as a reference the magnetic moment of ^{175}Lu, $\mu_I(^{175}\mathrm{Lu}) = 2.2325(8)\,\mu_\mathrm{N}$. This is the mean value from measurements of Brenner et al. [16] using the ABMR technique and of Müller et al. [17] using optical pumping of Lu^+. The relation

$$\frac{\mu_I}{IA} = \frac{{\mu_I}^{\mathrm{ref}}}{I^{\mathrm{ref}} A^{\mathrm{ref}}} \tag{2}$$

holds for any pair of isotopes, provided that hyperfine anomaly effects are negligible. These effects arise from the distribution of magnetic dipole density over the nuclear volume (Bohr-Weisskopf effect), varying from isotope to isotope. They may affect s-electron contributions to the ratios of eq. (2) up to the order of one percent.

For the dsp configuration of the excited state, it is obvious that the magnetic hyperfine structure contains a large contact interaction term caused by the s-electron. On the other hand, the ground state is essentially formed by the ds^2 configuration, which means that the hyperfine structure is produced by a d-electron, apart from the admixture of other valence configurations and from core polarization. For the $^2D_{3/2}$ state Brenner et al. [16] found an anomaly of 0.02(15) % between ^{175}Lu and ^{176}Lu which is negligible in the present context. Therefore, whenever this was possible, we evaluated the magnetic moments from the A-factors of the atomic ground state, although these are smaller and thus less accurate than those of the excited state. Only for $^{161-165}$Lu and for the $I = 1/2$ isomers ^{167m}Lu, ^{169m}Lu and ^{171m}Lu the analysis of the spectra gave no meaningful independent ground-state A-factors. In these cases we have assumed an

Table 3: Magnetic dipole moments of lutetium isotopes obtained from the measured A-factors. Theoretical values are taken from Ekström [5] or calculated using the indicated Nilsson configurations.

Isotope	I	μ [μ_N]	Configuration	μ_{theo} [μ_N]	Ref.
161	$1/2^+$	0.223 (3)	$\pi[411]1/2$	0.07	
162	1^-	0.0553 (11)	$\pi[411]1/2$ $\nu[521]3/2$	-0.6	
163	$1/2^+$	0.0769 (10)	$\pi[411]1/2$	0.02	
164	1^-	0.0591 (11)	$\pi[411]1/2$ $\nu[521]3/2$	-0.8	
165	$1/2^+$	-0.0245 (3)	$\pi[411]1/2$	-0.03	
166	6^-	2.912 (12)	$\pi[404]7/2$ $\nu[523]5/2$	2.74	
$166m_1$	3^-	0.189 (5)	$\pi[411]1/2$ $\nu[523]5/2$	0.33	
$166m_2$	0^-	0	$\pi[402]5/2$ $\nu[523]5/2$	0	
167	$7/2^+$	2.325 (4)	$\pi[404]7/2$	2.22	
167m	$1/2^+$	-0.0999 (13)	$\pi[411]1/2$	-0.05	
168	6^-	3.016 (25)	$\pi[404]7/2$ $\nu[523]5/2$	2.78	
168m	3^+	1.221 (5)	$\pi[541]1/2$ $\nu[523]5/2$	0.91	
169	$7/2^+$	2.295 (4)	$\pi[404]7/2$	2.21	
		2.297 (13)			[7]
169m	$1/2^-$	0.538 (7)	$\pi[541]1/2$	0.70	
170	0^+	0	$\pi[404]7/2$ $\nu[633]7/2$	0	
171	$7/2^+$	2.293 (4)	$\pi[404]7/2$	2.21	
		2.305 (12)			[7]
171m	$1/2^-$	0.585 (7)	$\pi[541]1/2$	0.72	
172	4^-	2.900 (10)	$\pi[404]7/2$ $\nu[521]1/2$	2.53	
		2.893 (15)			[7]
172m	1^-	1.98 (4)	$\pi[404]7/2$ $\nu[512]5/2$	1.79	
173	$7/2^+$	2.2805 (23)	$\pi[404]7/2$	2.21	
		2.280 (12)			[7]
174	1^-	1.988 (5)	$\pi[404]7/2$ $\nu[512]5/2$	1.79	
174m	6^-	1.492 (16)	$\pi[404]7/2$ $\nu[512]5/2$	1.80	
		1.497 (10)			[18]
175	$7/2^+$	2.2325 (8)[a]	$\pi[404]7/2$	2.20	[17, 16]
176	7^-	3.162 (12)	$\pi[404]7/2$ $\nu[514]7/2$	3.20	
		3.1692 (45)			[16]
176m	1^-	0.311 (7)	$\pi[404]7/2$ $\nu[514]7/2$	0.40	
		0.3185 (6)[b]			[4]
177	$7/2^+$	2.239 (7)	$\pi[404]7/2$	2.20	
		2.2384 (14)[b]			[3]
177m	$23/2^-$	2.308 (11)	$\pi[404]7/2 \begin{cases} \nu[514]7/2 \\ \nu[624]9/2 \end{cases}$	2.50	
		2.337 (13)			[7]
178	1^+	-1.377 (9)	$\pi[404]7/2$ $\nu[624]9/2$	-1.48	
178m	9^-	4.834 (9)	$\pi[514]9/2$ $\nu[624]9/2$	4.69	
179	$7/2^+$	2.375 (12)	$\pi[404]7/2$	2.20	

[a] Reference value.
[b] Recalibrated from A-factors measured by ABMR.

additional error of 1 % as to account for the unknown hyperfine structure anomaly[2)].

The magnetic moments[3)], together with earlier results, are collected in Table 3. It turns out that all recently published magnetic moments from low-temperature nuclear orientation experiments by König et al. [7] and Hinfurtner et al. [18] agree nearly perfectly with the present results. The insufficiencies of some results of the earlier nuclear orientation work have obviously been removed by using magnetic resonance techniques. The parities given in Table 3 in connection with the magnetic moments correspond to the assignment of Nilsson orbitals as explained in Section 5.

The spectroscopic quadrupole moments Q_S are evaluated from the relation:

$$\frac{Q_S}{B} = \frac{{Q_S}^{\mathrm{ref}}}{B^{\mathrm{ref}}} \,, \tag{3}$$

where B is the measured B-factor and ${Q_S}^{\mathrm{ref}}$ is the quadrupole moment of the reference isotope ^{175}Lu, $Q(^{175}\mathrm{Lu}) = 3.49(2)$ b, obtained by Dey et al. from X-ray transitions in muonic atoms [19]. The B-factors were taken from the hyperfine structure of the ground state where they are larger than in the excited state.

On the assumption that all nuclei are well deformed one can calculate the intrinsic quadrupole moments Q_0 by using the strong-coupling projection formula

$$Q_0 = \frac{(I+1)(2I+3)}{3K^2 - I(I+1)} Q_S \,, \tag{4}$$

or in the usual cases of $K = I$

$$Q_0 = \frac{(I+1)(2I+3)}{I(2I-1)} Q_S \,. \tag{5}$$

Table 4 gives the spectroscopic quadrupole moments, including those from other work where they are available, and the intrinsic quadrupole moments calculated from these. Again the values published recently by König et al. [7] are in very good agreement with the present ones, demonstrating that magnetic resonance measurements on nuclei oriented in ferromagnetic host lattices with well defined electric field gradients give reliable quadrupole moments.

4 The Evaluation of $\delta\langle r^2 \rangle$

The isotope shift $\delta\nu_i^{A,A'} = \nu^{A'} - \nu^A$ between two isotopes A and A' for an atomic transition i is caused by the different mean square radii of the nuclear charge distribution $\delta\langle r^2 \rangle$ and the different nuclear recoil energy. It can thus be written [21]

$$\delta\nu_i^{A,A'} = \frac{m_{A'} - m_A}{m_{A'} m_A}(M_{n,i} + M_{s,i}) + E_i f(Z) \lambda^{A,A'} \,. \tag{6}$$

The first expression on the right-hand side of this formula describes the mass dependence. It is convenient to separate it into the (trivial) normal mass shift with the constant $M_{n,i} = \nu_i m_e$ and the specific mass shift which for $s^2 \rightarrow sp$ transitions is estimated to be $M_s = 0(1) \times M_n$.

[2)] More quantitative evidence for negligible anomaly effects in the ground-state hyperfine structure is obtained from the ratios between the A-factors of both states. These ratios are identical for all isotopes within the experimental errors of typically 0.1 % to 2 % determined by the ground-state A-factors.

[3)] The values from the present experiment quoted by König et al. [7] were preliminary results obtained from the A-factors of the excited state without consideration of the hyperfine structure anomaly.

Table 4: Spectroscopic quadrupole moments Q_s obtained from the measured B-factors, deduced intrinsic quadrupole moments Q_0 and deformation values β_2.

Isotope	I	$Q_s[b]$	$Q_0[b]$	β_2	Ref.
162	1	0.519 (8)	5.19 (8)	0.23	
164	1	0.608 (7)	6.08 (7)	0.26	
166	6	4.33 (4)	6.89 (7)	0.29	
$166m_1$	3	2.715 (21)	6.52 (5)	0.28	
167	7/2	3.275 (24)	7.02 (5)	0.30	
168	6	4.77 (6)	7.58 (9)	0.32	
168m	3	2.431 (19)	5.83 (5)[c]	0.25[c]	
169	7/2	3.480 (25)	7.46 (6)	0.31	
		3.42 (12)			[7]
171	7/2	3.525 (25)	7.55 (6)	0.32	
		3.38 (4)			[7]
172	4	3.80 (4)	7.46 (6)	0.31	
		3.79 (6)			[7]
172m	1	0.76 (3)	7.56 (25)	0.32	
173	7/2	3.531 (24)	7.57 (6)	0.31	
		3.56 (4)			[7]
174	1	0.773 (7)	7.73 (7)	0.32	
174m	6	4.80 (5)	7.63 (7)	0.32	
175	7/2	3.49 (2)[a]	7.47 (5)	0.31	[19]
		3.62 (9)			[20]
176	7	4.92 (5)	7.36 (6)	0.30	
		4.92 (3)			[16]
		5.07 (7)			[20]
176m	1	-1.450 (12)	7.25 (12)	0.30	
		-1.47 (1)[b]			[4]
177	7/2	3.386 (26)	7.26 (6)	0.30	
		3.39 (2)[b]			[3]
177m	23/2	5.71 (5)	7.33 (6)	0.30	
		5.2 (5)			[7]
178	1	0.708 (10)	7.08 (10)	0.29	
178m	9	5.39 (5)	7.39 (6)	0.30	
179	7/2	3.316 (30)	7.11 (7)	0.29	

[a] Reference value.
[b] From ABMR measurement of B-factors as recalibrated by Raghavan [6]
[c] Tentatively assuming the projection factor for $K = I$ (see text).

The second part is the field shift which is sensitive to the nuclear charge distribution. This is expressed by the nuclear parameter $\lambda^{A,A'}$ which contains an expansion in radial moments,

$$\lambda^{A,A'} = \delta\langle r^2\rangle^{A,A'} + \frac{C_2}{C_1}\delta\langle r^4\rangle^{A,A'} + \frac{C_3}{C_1}\delta\langle r^6\rangle^{A,A'} + ... \tag{7}$$

The coefficients C_i are available from calculations [22] showing that $\delta\langle r^2\rangle^{A,A'}$ is the dominant part and the higher-order terms contribute only about 4 %.
The electronic factor E_i was evaluated using the expression

$$E_i = \frac{\pi a_0^3\, \Delta_i |\Psi(0)|^2}{Z}\,. \tag{8}$$

Replacing $\Delta_i|\Psi(0)|^2$ by $\gamma_i|\Psi_{6s}(0)|^2$ (with γ_i the screening ratio), one can use the contact hyperfine interaction to calculate the electron density $|\Psi_{6s}(0)|^2$ according to [23]

$$\pi a_0^3 |\Psi_{6s}(0)|^2 = \frac{3A_{6s}(m_p/m_e)}{8R_\infty \alpha^2 g_I(1-\delta)(1-\epsilon)F_R}\,. \tag{9}$$

The input data $A_{6s} = 0.276(6)\mathrm{cm}^{-1}$ [24], $g_I = \mu_I/(\mu_K I) = (2/7)\mu(^{175}\mathrm{Lu})$, $\epsilon = 0.015$, $\delta = 0.058$ and $F_R = 1.821$ [25], and $\gamma_i = 0.68$ [21] yield $E_i = 0.289(6)$. Of course, an error for E_i including only the errors of experimental input parameters is not really meaningful. As it is difficult to give estimated errors for the theoretical quantities and the validity of the semi-empirical formulas, we subsume all these under a final 10 % scaling error of the radii differences obtained from the described semi-empirical procedure [21].

Finally $f(Z)$ gives the ratio of the so-called field shift constant $C^{A,A'}$ and the nuclear parameter $\lambda^{A,A'}$. This ratio has to be calculated theoretically, and as it turns out to be insensitive to details of the nuclear charge distribution, one chooses a reference nucleus of a uniformly charged sphere,

$$f(Z) = \frac{C^{A,A'}_{\mathrm{unif}}}{\lambda^{A,A'}_{\mathrm{unif}}}\,. \tag{10}$$

Blundell et al. [26] calculated $C^{A,A'}_{\mathrm{unif}}$ by solving the Dirac equation nearby the nucleus assuming a sharp radius $R = R_0 A^{1/3}$ ($R_0 = 1.2$ fm). The corresponding quantity $\lambda^{A,A'}_{\mathrm{unif}}$ is readily calculated using eq. (7).

The values for $\delta\langle r^2\rangle^{A,A'}$ can now be found from $\lambda^{A,A'}$ following the procedure used previously [27]. This takes into account that eq. (7) holds for spherical nuclei, whereas in the deformation contributions to $\lambda^{A,A'}$ the corrections for higher-order radial moments appear somewhat differently. Considering the small influence of these corrections one can use any current version of the droplet model (see Section 5) to disentangle the spherical and deformation parts in the procedure of evaluating finally the neutron number dependence of the mean square charge radii.

The experimental reference isotope ^{170}Lu (mass number A) has been chosen for the presentation of the results. These results for $\delta\langle r^2\rangle^{170,A'}$ are included in Table 2 which also contains the isotope shifts. The errors in $\delta\langle r^2\rangle$ add up from four different contributions: (*i*) The statistical errors of the isotope shifts obtained from the fits of the spectra and (*ii*) the systematic calibration errors of the measured acceleration voltages, translated into the frequency scale, are experimental errors which correspond to less than one unit in the last digit (i.e. 10^{-3} fm^2). They are negligible compared to the errors of the evaluation procedure. (*iii*) The errors due to the

specific mass shift ($(A-A') \times 10^{-3}$ fm^2) and (*iv*) the estimated errors from the electronic factor E_i (see above) are both subsumed under a general 10 % error to be applied to absolute values of $\delta\langle r^2\rangle^{A,A'}$. Relative values as well as all details in the behaviour of the radii, such as the odd-even staggering and the isomer shifts, only depend on the very small experimental errors given for the isotope shifts.

There is only one literature value for the difference of the mean square charge radii of two lutetium isotopes, namely ^{175}Lu and ^{176}Lu. This was extracted by Zimmermann et al. [9] from the isotope shift in the LuI transitions from $5d6s^2\ ^2D_{3/2}$ to $5d6s6p\ ^4F_{3/2}$ at 573.7 nm and from $5d6s^2\ ^2D_{5/2}$ to $5d6s6p\ ^4F_{5/2}$ at 605.5 nm. The result, $\delta\langle r^2\rangle^{175,176} = 0.022(5)\mathrm{fm}^2$, quoted by King to be "remarkably small" [28], is at variance with our present value of $\delta\langle r^2\rangle^{175,176} = 0.041(5)\ \mathrm{fm}^2$. This is neither caused by a measuring error nor by a principal inconsistency of the evaluation procedures. The discrepancy can just be traced to the erroneous neglect of the relativistic correction, i.e. the expression $F_R(1-\delta)(1-\epsilon)$, in the calculation of the electronic factor E_i [29].

5 Discussion

We will first discuss briefly the single-particle properties reflected in the spins and magnetic moments and then elaborate on the collective deformation properties that are observed independently in the quadrupole moments and in the isotope shifts.

Direct atomic spectroscopy measurements of nuclear spins were already reported by Ekström [5] for eleven longer-lived isotopes. For seven additional nuclear states investigated here, the spin assignments proposed from nuclear spectroscopy measurements are considered to be safe [30]. With the present experiment we have thus added the spins of another twelve nuclear ground states or isomers. With the exception of ^{161}Lu ($I = 1/2$) the (partly tentative) earlier spin assignments from nuclear spectroscopy are confirmed. No previous nuclear spin information was found in the literature for ^{164}Lu ($I = 1$) and for the new isomer ^{167m}Lu ($I = 1/2$). The half-life of this isomer can be estimated to be about a minute or longer, because the delay time of the ISOLDE tantalum target for rare-earth elements is of this order, and the intensity of the $I = 1/2$ lines, compared to those of the $I = 7/2$ ground state, is apparently not reduced by decay during diffusion out of the target.

The magnetic dipole moments and the spins of Table 3 are shown in Figure 2. Data points associated with the same Nilsson orbitals are connected by solid lines. Predictions of the magnetic moments of the isotopes with mass numbers $A \geq 165$ were made by Ekström [5] on the basis of pure Nilsson states with effective g-factors $g_s = 0.6\ g_s^{\mathrm{free}}$, $g_{lp} = 1.00$, $g_{ln} = 0$, $g_R = 0.4$. We have extended these calculations to all isotopes investigated here. For comparison, these theoretical values as well as the assumed Nilsson configurations are included in Table 3. The general fair agreement of the measured magnetic moments with the model predictions demonstrates the appearance of rather pure Nilsson states as expected for a region of well-developed nuclear deformation.

The parities given in Table 3 correspond to this model interpretation of the magnetic moments. With the exception of the lightest isotopes for which very little is known, these agree with current parity assignments [30].

We will further discuss the nuclear structure information that can be extracted from our results by using a graphical summary of the radii and the quadrupole moments which are both related to collective deformation properties. Figure 3 shows the changes in the mean square charge radii $\delta\langle r^2\rangle$ for the ground states as well as for the isomers with respect to the reference isotope ^{170}Lu. They can be interpreted in the frame of the droplet model including deformation [31]. This essentially means that two independent trends are reflected by the mean square charge

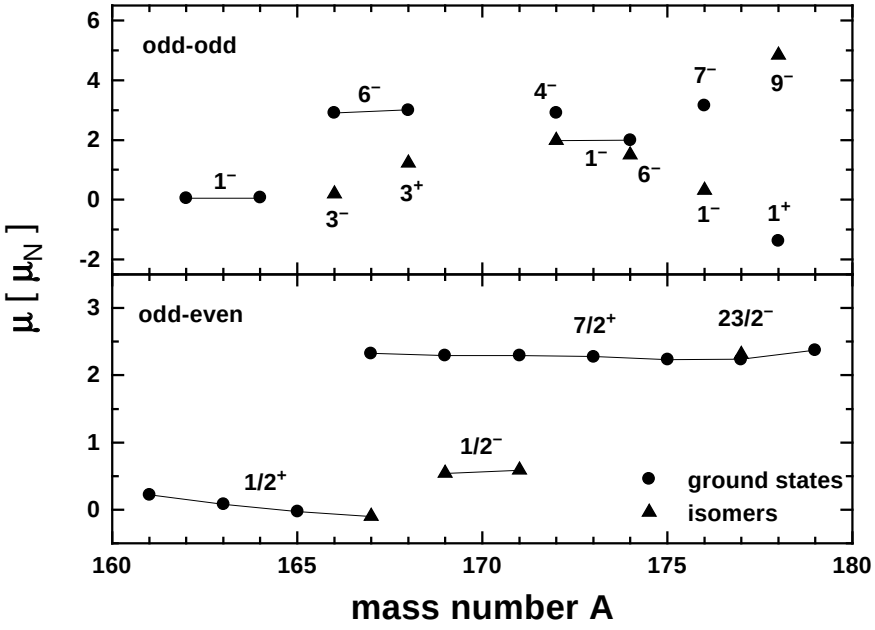

Figure 2: Spins I and magnetic moments μ. The parity assignments correspond to the Nilsson model states used to reproduce the magnetic moments. The values assigned to the same states are connected by thin lines.

radii plotted as a function of the neutron number: (*i*) The increase with the nuclear volume (assuming constant shape) is nearly linear and has about half the slope expected for identical proton and neutron distributions. In other words, the proton and neutron radii develop differently. (*ii*) Deformed shapes give an increased mean square radius compared to a spherical nucleus of the same volume. In the simplest parametrization of a liquid drop with a sharp radius,

$$\langle r^2 \rangle_\beta = \langle r^2 \rangle_0 \left(1 + \frac{5}{4\pi} \langle \beta^2 \rangle \right) , \tag{11}$$

one can put the $\delta\langle r^2 \rangle$ curve on a grid of parallel isodeformation lines. Apart from higher-order corrections the deformed droplet model formula [31] has essentially the structure of eq. (11). Choosing the recent "finite range" version of the droplet model [32], and assuming the quadrupole deformation $\beta_2 = 0.31$ for the stable ^{175}Lu (see below), we find a gradual increase of deformation from $\beta_2 \approx 0.2$ for the light isotopes just above $N = 90$ to $\beta_2 \approx 0.3$ for the isotopes with $N \geq 97$. The dashed curve of Figure 3 shows a theoretical prediction for the radii obtained from the finite range droplet model including β_2 and β_4 values as calculated by Möller et al. [32]. Although the values of β_4 (reaching -0.1) are quite appreciable, it turns out that for negative β_4 their contribution is almost negligible, due to the cancellation of the higher-order terms in the expression for the radii.

The representation of the radii given in Figure 3 suggests a development of deformation which is very well reproduced by the quadrupole deformation parameters β_2 deduced from the intrinsic quadrupole moments Q_0. These are shown in Figure 4, calculated again using the droplet model formulas [31]. The values of β_2 that correspond to the experimental changes in mean square charge radii $\delta\langle r^2 \rangle$ within the droplet model description are represented by the dotted curve. To be exact, the spherical droplet model contribution was subtracted from the experimental values of $\delta\langle r^2 \rangle$, and the remaining deformation contribution was corrected for

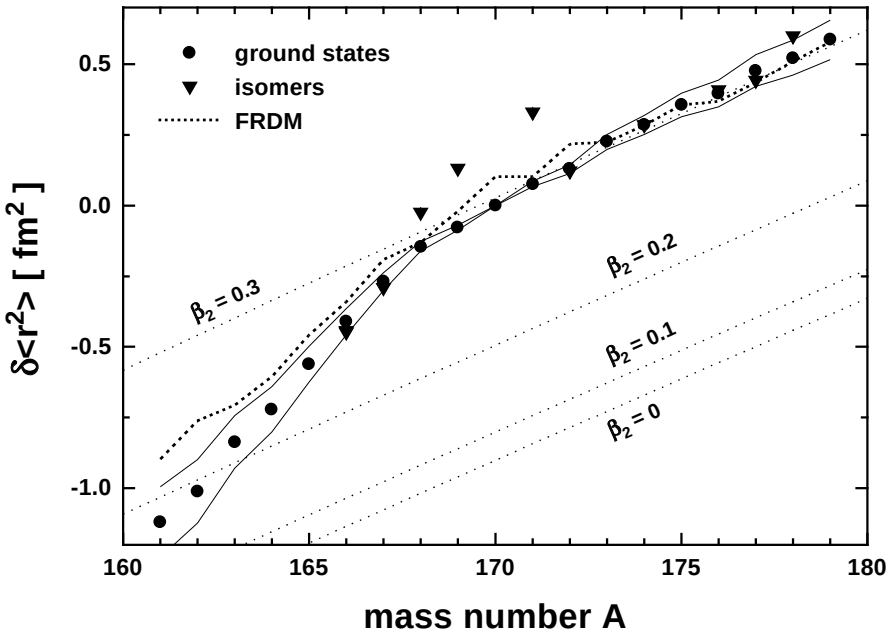

Figure 3: Changes in the mean square charge radii $\delta\langle r^2\rangle$. The calibration uncertainty is represented by the area between the two enveloping lines. The theoretical prediction (FRDM) and the isodeformation lines are based on the finite-range droplet model [32].

theoretical values of β_4, in order to extract β_2. Here again, the consideration of β_4 has very little influence on the results.

Pronounced deviations from the smooth $\delta\langle r^2\rangle$ curve towards larger radii are found for the isomers ^{169m}Lu and ^{171m}Lu with $I = 1/2$ and ^{168m}Lu with $I = 3$. This behaviour may be ascribed to an enhanced deformation which is not observable in a spectroscopic quadrupole moment for the $I = 1/2$ cases. The $1/2^-$ states forming these isomers are associated with a proton configuration arising from the $[541]1/2$ intruder Nilsson orbital. An enhanced deformation for this configuration from the $h_{9/2}$ shell was predicted by Nazarewicz et al. [33]. In the odd-odd case of ^{168m}Lu the $1/2^-$ proton couples with a neutron in the $[523]5/2$ orbital to form the 3^+ state. This assignment is confirmed by the magnetic moment.

The intrinsic quadrupole moment of this 3^+ state as deduced from the spectroscopic quadrupole moment in the strong-coupling limit (with $K = I$ according to eq. (5)) is substantially smaller than expected from the overall systematics (see Figure 4). This can be related to a non-negligible Coriolis mixing that occurs when the intruder $\pi[541]1/2$ orbital coming down from the $h_{9/2}$ state couples with the $\nu[523]5/2$ orbital to both $K = 2$ and 3. The $K = 2$ admixture will alter the projection factor of eq. (5) thus leading to a higher value for Qo. This interpretation is consistent with the enhanced deformation increasing the radius for the ^{168m}Lu state as observed from the isomer shift. Recently, a similar manifestation in the quadrupole moments of the effect of strong Coriolis mixing due to the deformation-driving $\pi[541]1/2$ orbital was reported for the $I^\pi = 5^-$ ground states of ^{184}Ir and ^{186}Ir [34].

All other isomer shifts – those of the neutron-deficient ^{166,167}Lu and of the near-stable ^{174,176,177,178}Lu – are found to be very small. This is again consistent with the nearly identical values of the intrinsic quadrupole moments which are available for both nuclear states in all cases of $I > 1/2$. Considering the sensitivity of Q_0 to β_2 only and the sensitivity of $\delta\langle r^2\rangle$ to all multipole orders of deformation one concludes that the nuclear shape is very similar for the

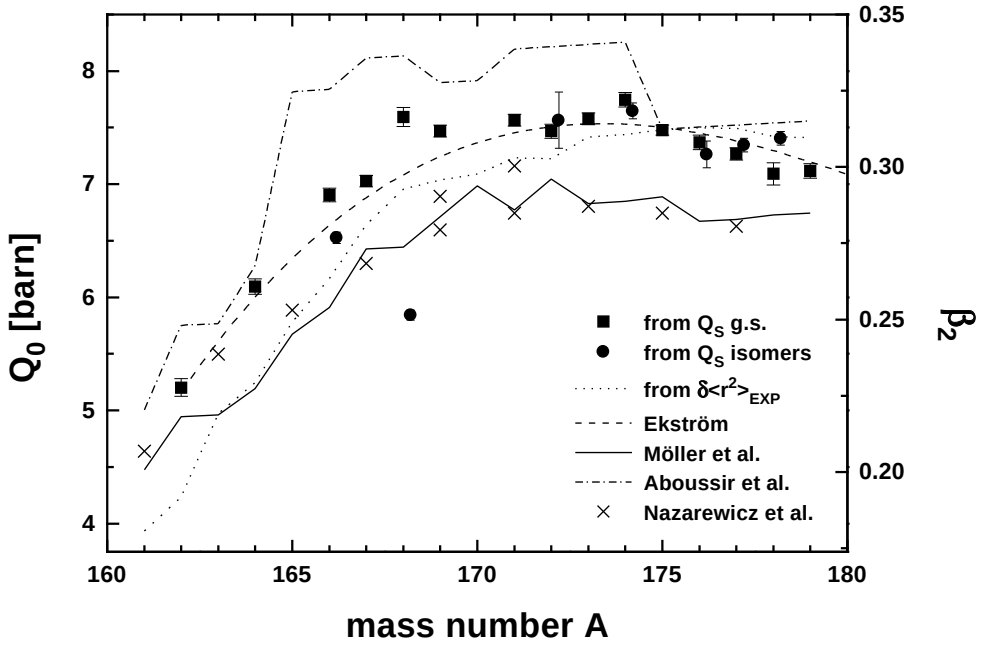

Figure 4: Intrinsic quadrupole moments Q_0 and quadrupole deformation parameters β_2 evaluated from the measured quadrupole moments (for ^{168m}Lu see discussion). Deformations corresponding to the experimental radii in the framework of the droplet model (FRDM) description are shown for comparison. Theoretical predictions are from different model calculations by Ekström [5], Möller et al. [32], Aboussir et al. [36] and Nazarewicz et al. [33].

high-spin and the low-spin states of the same nucleus. This fact is particularly remarkable in the case of ^{177}Lu, where a long-lived isomer with $I = 23/2$ coexists with the $I = 7/2$ ground state. The high spin of this isomer arises from the alignment of a neutron pair, and the isomer shift is only $-0.035(6)\,\mathrm{fm}^2$, corresponding to a change in deformation of less than 0.01. Adding one proton to this state leads to ^{178}Hf with the $I = 16$ isomer ^{178m2}Hf which was recently investigated by Boos et al. [35]. They found a similarly small isomer shift of $-0.059(9)\,\mathrm{fm}^2$ for this case.

Although the individual spectroscopic quadrupole moments seem to scatter randomly, the intrinsic ones calculated using eq. (4) lie on a smooth curve. Thus the information about the quadrupole moments contained in Figure 4 includes the validity of the strong-coupling scheme. The negative sign of the spectroscopic quadrupole moment of ^{176m}Lu is due to a particular combination of the angular momentum quantum numbers, namely $K = 0$ and $I = 1$, leading to a negative projection factor, and does not indicate an oblate shape. For all nuclei except ^{168m}Lu and ^{176m}Lu the assumption $K = I$ is valid.

Several theoretical predictions of the behaviour of deformation over the whole series of lutetium isotopes are available. In Figure 4 these theoretical values of β_2 are compared to the experimental values given by the intrinsic quadrupole moments Q_0. The dashed curve in this figure, following essentially the measured values, shows the theoretical equilibrium deformations calculated by Ekström using the Strutinsky shell-correction method on the basis of the Nilsson model [5]. The solid curve shows the corresponding deformation values from a recent theoretical approach based on the finite-range droplet model (FRDM) [32]. A third approach [36], based on the extended Thomas-Fermi plus Strutinski integral method (ETFSI), is represented by the dashed-dotted line. While the earliest prediction reproduces the experimental data nearly

quantitatively, the results of the recent calculations either underestimate (FRDM) or overestimate (ETFSI) generally the absolute values of β_2. This may be explained by the different scope of the theoretical approaches. The FRDM and the ETFSI calculations aim at a coherent description of nuclear properties over the entire chart of nuclides, whereas the calculations by Ekström use Nilsson model parameters that are proven appropriate to describe nuclei in the rare-earth region. The most detailed calculation of the deformation properties of odd-Z rare-earth nuclei [33], on the other hand, predicts a deformation maximum of only 0.26 for the $7/2^+$ proton state forming the ground state of the even-N isotopes. However, for the assumed Woods-Saxon potential the deformation of the resulting charge distribution should be about 10 % larger than the calculated deformation of the average field [33, 37]. This correction has been included in the values shown in Figure 4. Tracing the reasons for the remaining discrepancy between the theoretical maximum of 0.28 and the experimental one of 0.32 would require a more careful theoretical treatment of the real observables. Nevertheless, all theoretical predictions show the proper general trends of the experimental curve including a deformation increase in the light isotopes up to neutron number $N \approx 100$ and a slight decrease towards the heaviest isotopes.

6 Conclusion

The present laser spectroscopy measurements on lutetium ($Z = 71$) isotopes cover the range of neutron numbers between $N = 90$ and 108 with 30 nuclear states of half-lives above 1 minute. A most striking feature of the results is the remarkable consistency in the description of different observables within the same model. The deformation properties reflected in the mean square charge radii can be directly identified with those extracted from the quadrupole moments. This means that the strong-coupling projection formula holds to a very good approximation. Concerning the droplet-model decomposition of the radii there is some arbitrariness in the choice of the parameters which essentially affects the slope of the volume part $\langle r^2 \rangle_0$. On the other hand, a similar uncertainty of the order of 10 % is introduced into the slope of the experimental $\delta\langle r^2 \rangle$ curve by the evaluation procedure. In fact, the consistency of the interpretation goes beyond these uncertainties. By adjusting the parameters of the spherical droplet model to the deformation values of only two isotopes one would reproduce the full curve without any remaining freedom.

This gives confidence that our description of the deformation properties is quite realistic even in details. The general trend corresponds to an increase from $\beta_2 \approx 0.2$ for ^{161}Lu ($N = 90$) towards a maximum of $\beta_2 \approx 0.32$ around ^{174}Lu ($N = 103$) followed by a slight decrease towards the neutron-rich isotopes.

These observations as well as the spins and magnetic moments of single-particle states fit very well to the theoretical expectations which are essentially based on the shell correction calculations of equilibrium shapes and the Nilsson orbitals occupied by the unpaired proton. We conclude that in regions of well developed deformation, unlike in transitional regions close to magic neutron or proton numbers, the ground-state gross properties behave in many details as expected from rather global models.

We wish to thank E. Hagn for valuable discussions and for the exchange of preliminary material. This work has been funded by the German Federal Minister for Research and Technology (BMFT) under the contract number 06 MZ 188 I.

References

[1] R. Neugart, in Lasers in Nuclear Physics (eds. C.E. Bemis, Jr., and H.K. Carter), Nuclear Science Research Conf. Series, Vol. 3, Harwood, Chur-London-New York (1982), p. 231

[2] E.W. Otten, in Treatise on Heavy-Ion Science, Vol. 8, editor D.A. Bromley, Plenum Press, New York (1989), p.517
[3] F.R. Petersen and H.A. Shugart, Phys. Rev. **126** (1962) 252
[4] M.B. White, S.S. Alpert, S. Penselin, T.I. Moran, V.W. Cohen and E. Lipworth, Phys. Rev. **137** (1965) B 477
[5] C. Ekström, Physica Scripta **13** (1976) 217
[6] P. Raghavan, At. Data Nucl. Data Tables **42** (1989) 189
[7] C. König, B. Hinfurtner, E. Hagn, E. Zech and R. Eder, Phys. Rev. **C 54** (1996) 1027
[8] W. Borchers, U. Georg, A. Klein, P. Lievens, R. Neugart, M. Neuroth, Pushpa M. Rao and Ch. Schulz, Proc. 6th Int. Conf. on Nuclei far from Stability & 9th Int. Conf. on Atomic Masses and Fundamental Constants, Bernkastel-Kues 1992, eds. R. Neugart and A. Wöhr, Inst. Phys. Conf. Ser., Vol. 132, IOP Publishing, Bristol (1993), p. 213
[9] D. Zimmermann, P. Zimmermann, G. Aepfelbach and A. Kuhnert, Z. Phys. **A 295** (1980) 307
[10] A. Nunnemann, D. Zimmermann and P. Zimmermann, Z. Phys. **A 290** (1979) 123
[11] T. Bjørnstad, E. Hagebø, P. Hoff, O.C. Jonsson, E. Kugler, H.L. Ravn, S. Sundell, B. Vosicki and the ISOLDE Collaboration, Nucl. Instr. Meth. **B 26** (1987) 174
[12] A.C. Mueller, F. Buchinger, W. Klempt, E.W. Otten, R. Neugart, C. Ekström and J. Heinemeier, Nucl. Phys. **A 403** (1983) 234
[13] A.H. Wapstra, G. Audi and R. Hoekstra, At. Data Nucl. Data Tables **39** (1988) 281
[14] F. James, M. Roos, MINUIT long-write-up, CERN Computer Center, Program Library, CERN, Geneva (1977)
[15] R. Engleman, Jr. R.A. Keller and C.M. Miller, J. Opt. Soc. Am. **B 2** (1985) 897
[16] T. Brenner, S. Büttgenbach, W. Rupprecht and F. Träber, Nucl. Phys. **A 440** (1985) 407
[17] R. Müller and E.W. Weber, Z. Phys. **A 275** (1975) 305
[18] B. Hinfurtner, E. Hagn, E. Zech, R. Eder, J. Kern and ISOLDE Collaboration, Phys. Lett. **B 263** (1991) 29
[19] W. Dey, P. Ebersold, H.J. Leisi, F. Scheck, H.K. Walter and A. Zehnder, Nucl. Phys. **A 326** (1979) 418
[20] B. Olaniyi, A. Shor, S.C. Cheng, G. Dugan and C.S. Wu, Nucl. Phys. **A 403** (1982) 572
[21] P. Aufmuth, K. Heilig and A. Steudel, At. Data Nucl. Data Tables **37** (1987) 455
[22] E.C. Seltzer, Phys. Rev. **188** (1969) 1916
[23] H. Kopfermann, Nuclear Moments, Academic Press, New York (1958)
[24] F. Wyart, Physica Scripta **18** (1978) 87
[25] S.A. Blundell and C.W.P. Palmer, J. Phys. **B 21** (1988) 3809
[26] S.A. Blundell, P.E.G. Baird, C.W.P. Palmer, D.N. Stacey, G.K. Woodgate and D. Zimmermann, Z. Phys. **A 321** (1985) 31
[27] S.A. Ahmad, W. Klempt, R. Neugart, E.W. Otten, P.-G. Reinhard, G. Ulm and K. Wendt, Nucl. Phys. **A 483** (1988) 244
[28] W.H. King, Isotope Shifts in Atomic Spectra, Plenum Press, New York (1984)
[29] D. Zimmermann, private communication
[30] R.B. Firestone, Table of Isotopes, V.S. Shirley, editor, John Wiley & Sons, New York (1996)
[31] W.D. Myers and K.-H. Schmidt, Nucl. Phys. **A 410** (1983) 61
[32] P. Möller, J.R. Nix, W.D. Myers and W.J. Swiatecki, At. Data Nucl. Data Tables **59** (1995) 185
[33] W. Nazarewicz, M.A. Riley and J.D. Garrett, Nucl. Phys. **A 512** (1990) 61

[34] G. Seewald, E. Hagn, B. Hinfurtner, E. Zech, D. Forkel-Wirth, R. Eder and ISOLDE Collaboration, Phys. Rev. Lett. 77 (1996) 5016
[35] N. Boos, F. Le Blanc, M. Krieg, J. Pinard, G. Huber, M.D. Lunney, D. Le Du, R. Meunier, M. Hussonnois, O. Constantinescu, J.B. Kim, Ch. Briançon, J.E. Crawford, H.T. Duong, Y.P. Gangrski, T. Kühl, B.N. Markov, Yu.Ts. Oganessian, P. Quentin, B. Roussière and J. Sauvage, Phys. Rev. Lett. **72** (1994) 2689
[36] Y. Aboussir, J.M. Pearson, A.K. Dutta and F. Tondeur, At. Data Nucl. Data Tables **61** (1995) 127
[37] J. Dudek, W. Nazarewicz and P. Olanders, Nucl. Phys. **A 420** (1984) 285